A Study of End Face Geometry and Visual Inspection of a Very Small Form Factor Ferrule

Ian Dancel, Samuel Field, Madison Good, Michael Kadar-Kallen, Sharon Lutz, Dirk Schoellner, Charlie Stroup

US Conec Ltd., Hickory, North Carolina

+1-828-323-8883 · sharonlutz@usconec.com

Abstract

This paper studies the end face geometry and visual quality of a multi-fiber VSFF connector, the MMC connector with TMT ferrule, using traditional parameters defined in IEC standards. Data from a wide-ranging sample set of MMC connectors is gathered for this study, comparing end face geometry and visual quality of samples to optical performance. End face geometry measurements including minus coplanarity, ferrule surface radii, fiber tip spherical radii, ferrule surface angles, and fiber heights are presented along with corresponding optical loss measurements. Currently, no standard exists defining limits for end face geometry for multi-fiber connectors with fiber counts greater than 12; therefore, this wide-ranging data set can be used to begin establishing baseline criteria for critical end face geometry features for the multi-fiber ferrule.

Keywords: MT; TMT; MPO-16, MMC; multi-fiber connector; VSFF; density; visual inspection; end face geometry; endface; EFG.

1. Applications / Background

Growing hyperscale and artificial intelligence data center architecture demands are driving corresponding increases in bandwidth capabilities that provide density challenges for legacy optical connectors. A new connector design that leverages the well-known stability, reliability, and longevity of traditional MPO connectors, while dramatically reducing the connector footprint, is necessary to meet the bandwidth demands of modern networks and achieve the density required to support these networks. This paper reviews the development and testing of a new multi-fiber very small form factor (VSFF) connector, the MMC connector with TMT ferrule [1]. While multiple fiber count variants of the TMT ferrule are available, unless otherwise specified, for this paper 16 fiber count ferrules were used.

2. Connector Information

The MMC connector is a new VSFF multi-fiber connector which utilizes a new ferrule as well, the TMT ferrule. Shown in Figure 1, the TMT ferrule is two-thirds the height and half the length of the traditional MT ferrule. It was designed such that the precision optical and mechanical tolerances are compliant with the MT optical interface IEC 61755-3-31 for Grade B performance [2]. The TMT ferrule is designed without the ferrule shoulder and epoxy window that are present on traditional MT ferrules. The elimination of such features not only enables the reduced footprint of the TMT ferrule but allows the incorporation of two sets of asymmetric flanges on each corner edge of the ferrule face, resulting in a keyed ferrule to eliminate ferrule misalignment and simplify polarity management, termination, and deployment.

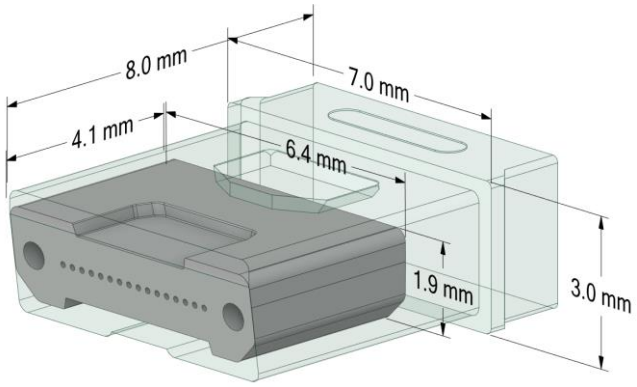

Figure 1. The TMT ferrule is two-thirds the height and half the length of a traditional MT ferrule

Compliance with MT-based standards is an important feature of the TMT ferrule, enabling mating compatibility between TMT and MT ferrules [3]. This is achieved by utilizing the same 250 µm pitch between fiber channels in the ferrule, as well as using the same pitch and diameter for guide bore mating features (see Figure 2).

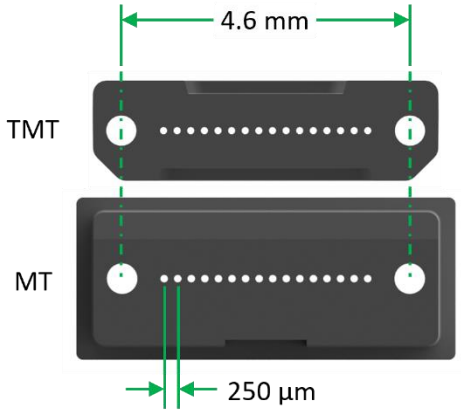

Figure 2. The TMT and MT ferrules have the same guide bore features and fiber pitch for interoperability

The MMC connector takes advantage of the reduced TMT ferrule footprint and can achieve three times the density of an MPO connector (Figure 3).

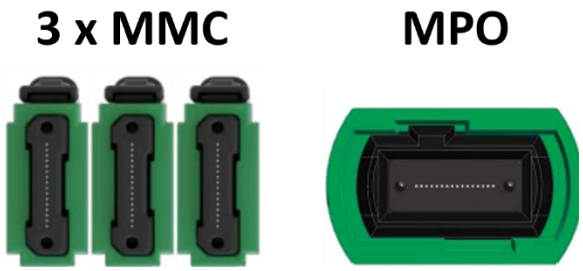

Figure 3. The MMC connector body can achieve three times the density of a traditional MPO connector

Building on the TMT ferrule design, the MMC connector housing features an internal and external railing system, where the internal railing ensures that the TMT ferrule can only be installed into the connector in one orientation. This simplifies polarity and termination. The external rail system of the MMC connector is also asymmetrical so that the connector can only be installed into an adapter in one orientation. The MMC adapters are designed around the connector rail system and prevent improper installation of the assembly. The railing system on the connector and adapter creates a significantly larger and longer contact area between the components than prior connector designs, and therefore provides an improved pre-alignment between the connector components prior to the ferrules coming together. The latching mechanism to hold the connectors into the adapter has been moved to the outside of the connector body, as can be seen in the top of Figure 4. By moving the latching away from the ferrule end face, a source of potential debris generation in prior connector designs has been mitigated.

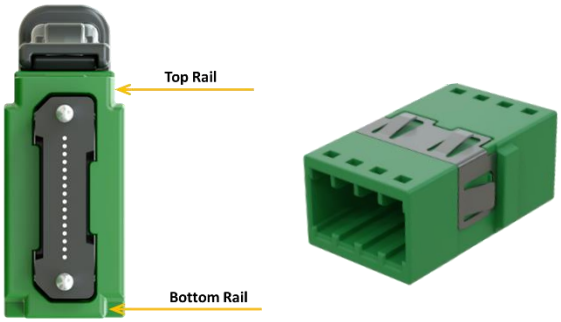

Figure 4. MMC connector and adapter rail system

3. Relevant Standards & Definitions

With new connector development, existing standards are referenced for critical parameters pertaining to physical contact. The MMC connector with TMT ferrule can be validated and tested using standard industry procedures for multi-fiber connectors, including the use of end face geometry (EFG) measurements using an interferometer and insertion loss testing. The specification limits for the EFG parameters evaluated in this paper are based on the tolerances for 12-fiber angled singlemode MT ferrules defined in IEC-61755-3-31 [2] in order to be consistent with existing industry knowledge and practices. The IEC limits were developed using historical empirical data, as well as modeling. These tolerances are summarized in Table 1. Note that curvatures of the fiber and ferrule in this table are defined by multiplying the inverses of the radii of curvature by 1 meter to form dimensionless parameters that have well-defined lower and upper bounds.

Table 1. End face geometry limits

Symbol	Description	Min	Max	Units
CF	Minus Coplanarity	0	400	nm
SX	Ferrule X-Angle	-0.15	0.15	°
SY	Ferrule Y-Angle	7.8	8.2	°
H	Fiber Height	1000	3500	nm
RF	Fiber Tip Radius	1	-	mm
1 m / RF	Fiber Tip Curvature	0	1000	-
RX	Ferrule X-Radius	> 2000 or < -10000		mm
1 m / RX	Ferrule X-Curvature	-0.1	0.5	-
RY	Ferrule Y-Radius	5	-	mm
1 m / RY	Ferrule Y-Curvature	0	200	-

4. End Face Geometry Data

In order to establish baseline performance data on the new connector system, ferrules were sampled from production every day for several months and were terminated using standard procedures [4-9] using multiple operators. During this testing, multiple interferometers were used as well. The end face geometry test procedure included a deliberate re-measurement of the first ferrule that is tested from each batch of parts. This provided a set of data to evaluate the repeatability of EFG measurements in a production setting. For example, if there are 6 ferrules in a batch of parts to be measured, then ferrules 1, 2, 3, …, 6 are measured, followed by a re-measurement of ferrule 1. The difference between the measurements of ferrule 1 at the beginning and end of the batch has a random error that is $\sqrt{2}$ times the repeatability of the measurement of a single ferrule. Table 2 summarizes the repeatability (6 standard deviations) of the measurements of relevant end face geometry parameters. The total tolerance shown in Table 2 is equal to Max – Min from Table 1.

Table 2. End face geometry repeatability (6σ) compared to the total tolerance

Symbol	6σ	Units	6σ / Tot. Tol.
CF	26	nm	6%
SX	0.16	°	55%
SY	0.13	°	32%
H	56	nm	2%
1m / RF	20	-	2%
1m / RX	0.04	-	6%
1m / RY	0.24	-	0.12%

Figure 5 demonstrates the distribution of the differences in the ferrule Y-angle (SY) between the first and last measurements in a batch. The limits of ± 0.4° on the horizontal axis are the worst-case differences allowed by the tolerance 8° ± 0.2° specified in Table 1.

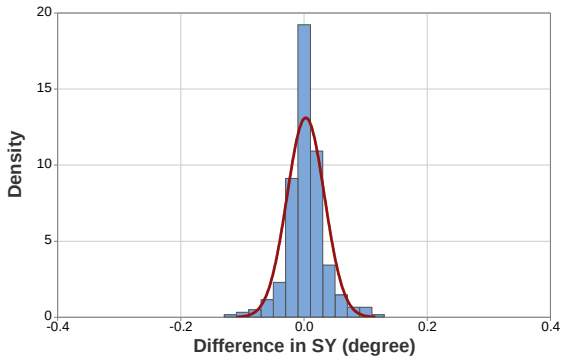

Figure 5. Difference in ferrule surface Y-angle (SY) between the first and last measurements in a batch

Figures 6 through 8 illustrate the ferrule surface angles and minus coplanarity for all samples measured in production over the same time period as the repeatability samples. In cases where a sample was measured more than once, the first measurement data is displayed. The IEC specifications for 12F MT ferrules (Table 1) are included for reference as vertical lines.

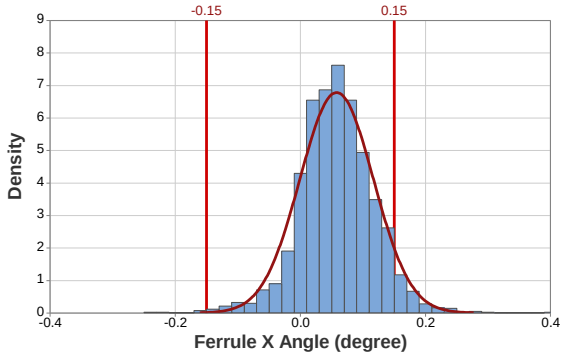

Figure 6. Histogram of the ferrule surface X-angle (SX).

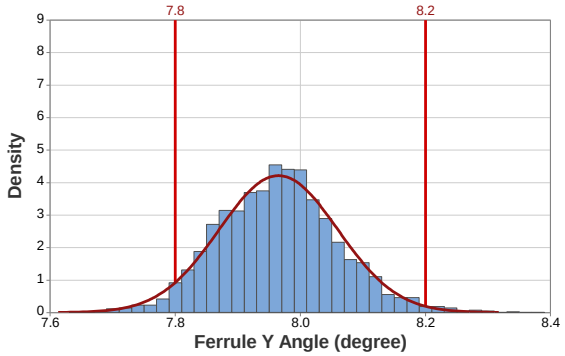

Figure 7. Histogram of the ferrule surface Y-angle (SY)

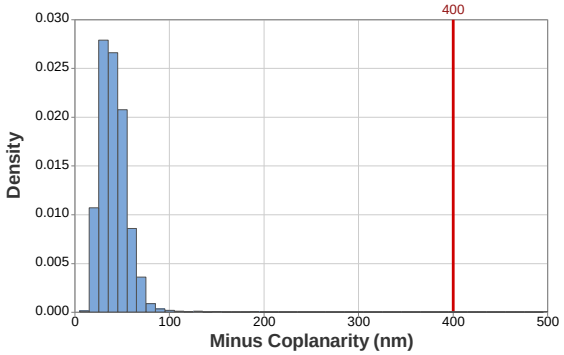

Figure 8. Histogram of the minus coplanarity (CF)

In cases where the ferrule surface angles are measured to be outside the specification limits the ferrules are re-measured, typically resulting in passing results, as it is important to note that all data in Figures 6 through 8 are the first pass data before additional cleaning and remeasurement.

Insertion loss was measured to demonstrate the performance of the ferrule as part of the process. Connectors were intermated to every other ferrule pulled from the same sample batch during the sampling period, but due to the sheer volume of testing that would be required, were not intermated across multiple batches. Figure 9 shows a histogram of the insertion loss for the connectors whose EFG values are shown in the figures above. Figure 10 graphs the cumulative distribution functions for this insertion loss data.

Figure 9. Insertion loss distribution at 1310 nm

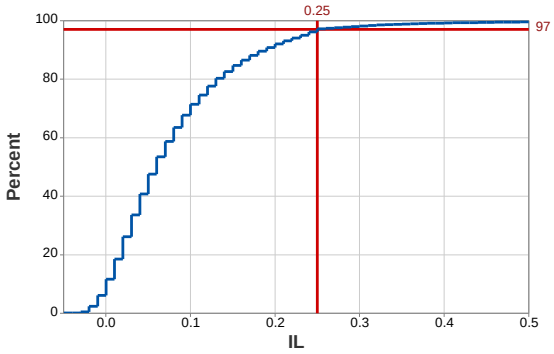

Figure 10. Cumulative distribution function for the insertion loss data shown in Figure 9

Note that distribution of insertion loss at 1310 nm is somewhat truncated at 0.25 dB. This is because ferrules are cleaned and re-mated once or twice if the loss exceeds 0.25 dB on any fiber. The data in Figure 9 and Figure 10 are the last insertion loss measurements for all mated pairs.

5. Ferrule Y-Angle Sensitivity

IEC 61755-3-31 [2] specifies the ferrule Y-angle (SY) to be 8.0° ± 0.2°, which allows for a 0.4° total range for SY. This IEC standard defines EFG limits of angled MT ferrules with a single row of up to 12 fibers. It is used as a point of reference in this paper for TMT ferrules with a single row of 16 fibers.

A test was conducted to determine the sensitivity of the TMT ferrule insertion loss (IL) performance when a mated pair of ferrules has a difference in ferrule Y-angle (ΔSY) of up to 0.4° and to determine at what point ΔSY becomes large enough that the fiber cores of the mated pair no longer maintain physical contact. If mating connectors have ferrule surface Y-angles of SY1 and SY2, then ΔSY is defined as

$$\Delta SY = |SY1-SY2| \qquad \text{(Equation 1)}$$

A set of 24 1x16 TMT ferrules were polished in such a way as to produce ferrules with a deliberately wide range of SY values. EFG for all ferrules were measured; average values are shown in Table 3. The TMT ferrules were then connectorized using MMC hardware. Three MMC connectors were chosen to be pinned, and the remaining 21 connectors were unpinned. The test consisted of mating all 21 unpinned connectors to each of the pinned connectors resulting in 63 mated pair combinations. IL was measured at 1310 nm and 1550 nm. The three pinned connectors were chosen such that the resulting ΔSY between mated pairs ranged from 0.11° to 1.24°.

Table 3. EFG parameters and average measured values

Symbol	Description	N	Average	Units
CF	Minus Coplanarity	24	36	nm
SX	Ferrule X-Angle	24	0.01	°
SY	Ferrule Y-Angle	24	7.03	°
H	Fiber Height	384	1998	nm
RF	Fiber Tip Radius	384	5	mm
RX	Ferrule X-Radius	24	-15811	mm
RY	Ferrule Y-Radius	24	184	mm

The results show that 30 mated pairs meet the maximum IL criterion of 0.35 dB with an average IL of 0.087 dB at 1310 nm. The ΔSY of these mated pairs are ≤ 0.72°. Figure 11 shows the average IL at 1310 nm versus ΔSY. The other 33 mated pairs with ΔSY > 0.72° have higher average IL due to a lack of physical contact between fiber cores, which is evident in the wavelength dependent loss (WDL) scatter plot [10] of IL at 1310 nm and 1550 nm in Figure 12. By contrast, a scatter plot for the 30 passing mated pairs is shown in Figure 13. Figure 14 shows the percentage of mated pairs with WDL inside acceptable limits as a function of ΔSY. From these results, it is evident that a ΔSY ≤ 0.7° results in contact between the ferrules and acceptable insertion loss performance. Therefore, the current specification of 8.0° ± 0.2° has a safety margin for the connectors to still perform well even with other specification variations.

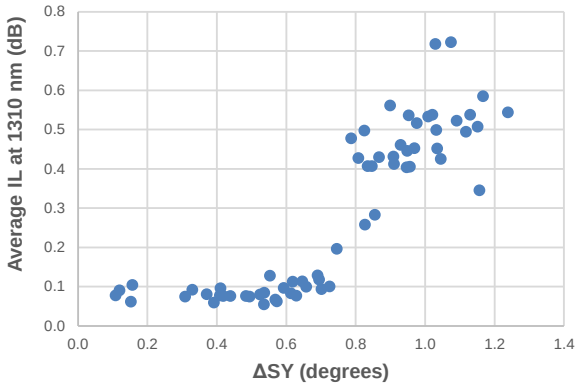

Figure 11. ΔSY of the mated pair and resulting IL average at 1310 nm

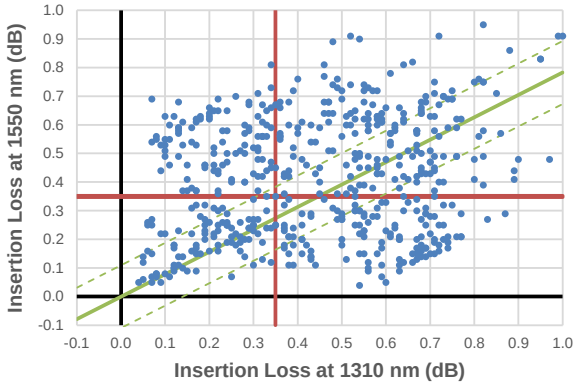

Figure 12. Wavelength dependent loss for mated pairs with ΔSY > 0.72°

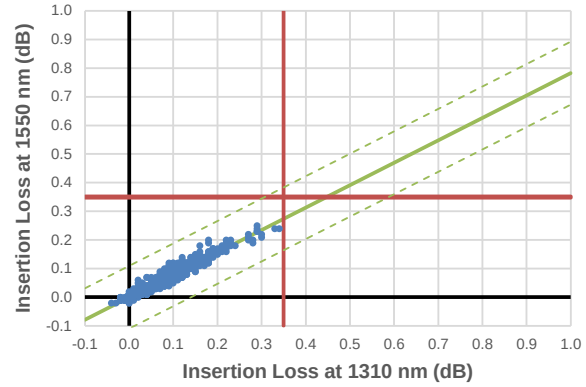

Figure 13. Wavelength dependent loss for mated pairs with ΔSY ≤ 0.72°

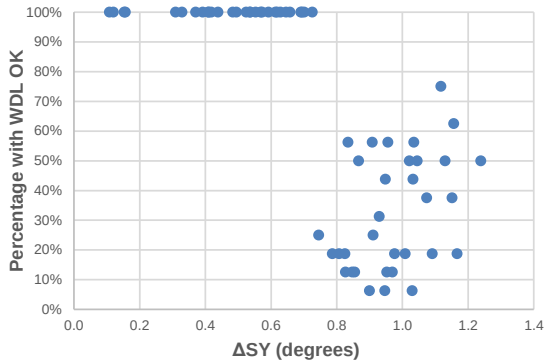

Figure 14. Percentage of mated pairs with wavelength dependent loss inside the limits (OK) as a function of the difference in ferrule Y-angles

6. Visual Inspection

Contamination and end face fiber defects on multi-fiber connectors has been linked to poor insertion loss and return loss (RL) performance. Contamination should be removed by utilizing typical cleaning methods. End face fiber defects are typically the result of damage during handling of the connector or during the polishing process. To study the effect of end face fiber defects on the TMT ferrule's performance, twelve 1x16 TMT/MMC to 1x16 MT/MPO subassemblies were constructed. The typical polishing process for the TMT ferrule is a 5-step process [9]. These TMT/MMC connector ends were polished using only the first 3 steps of the process, deliberately omitting the last 2 steps that have the greatest impact on end face quality. After polishing, the ferrule end face quality was inspected to IEC 61300-3-35 [11] for pass/fail grading. The worst examples from these twelve are provided in Figures 15, 16, and 17. The reduction in polishing steps had a minimal effect on the resulting end face geometry, as can be seen in Table 4. Due to the similarities in geometry, it can be reasoned that any reduction in performance during testing can be attributed to end-face defects and not the deviation from the typical polishing process.

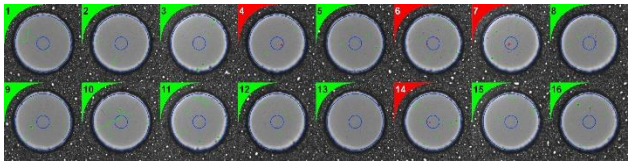

Figure 15. TMT ferrule #18 end face

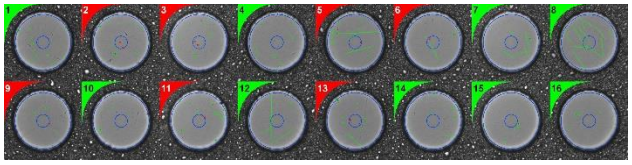

Figure 16. TMT ferrule #14 end face

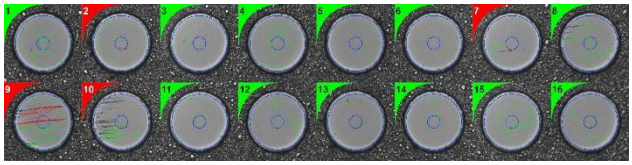

Figure 17. TMT Ferrule #10 End Face

Table 4. EFG For tested assemblies

Symbol	Description	N	Average	Units
CF	Minus Coplanarity	12	42	nm
SX	Ferrule X-Angle	12	0.10	°
SY	Ferrule Y-Angle	12	8.12	°
H	Fiber Height	192	2203	nm
RF	Fiber Tip Radius	192	7.94	mm
RX	Ferrule X-Radius	12	41842	mm
RY	Ferrule Y-Radius	12	190	mm

Six MMC connectors were chosen to be pinned, and the remaining six connectors were unpinned. The test consisted of mating all six unpinned connectors to each of the pinned connectors resulting in 36 mated pair combinations. The intermate results shown in Figure **18** demonstrate loss performance with an average IL of 0.05 dB and a maximum IL of 0.37 dB for wavelengths 1310 nm and 1550 nm. The intermate results shown in Figure 19 demonstrate return loss (RL) performance with an average RL of 66 dB and a minimum of 55 dB across wavelengths 1310 nm and 1550 nm.

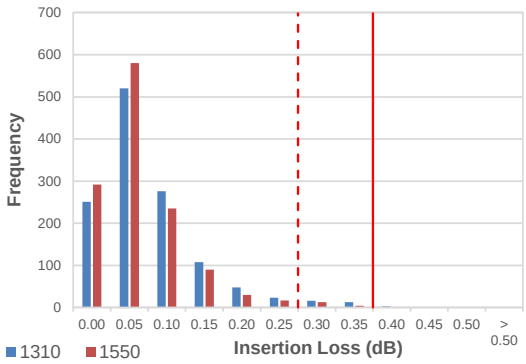

Figure 18. IL results for tested subassemblies

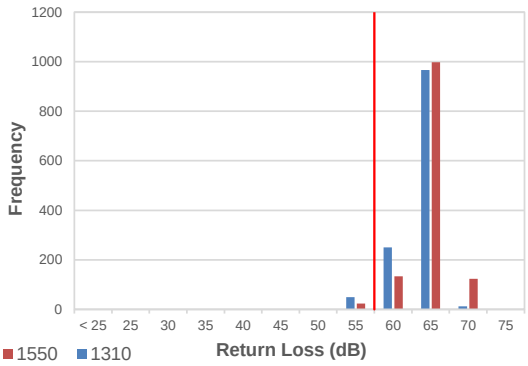

Figure 19. Return loss of tested sub-assemblies

There is no obvious correlation between small failing scratch/pits and connector performance for the TMT ferrule from these tests. Evaluation of the RL results shows that all ferrules except ferrule #12 have channels with a RL ≥ 60 dB at 1310 nm. Ferrule #12, whose end face pass rate results are presented in Figure 20, has an average RL of 57 dB at 1310 nm on channels 4 and 13 across all mates, despite having passing end face visuals on those channels.

Channels 4 and 13 saw an RL of 58 dB and 57 dB respectively when ferrule #12 was mated to ferrule #18. Both ferrules had passing end faces for channel 13, but still saw a lower RL than channel 4 which had a failing end face fiber. This mated pair shared a failing end face on channel 14 but was still able to achieve an RL of 64 dB.

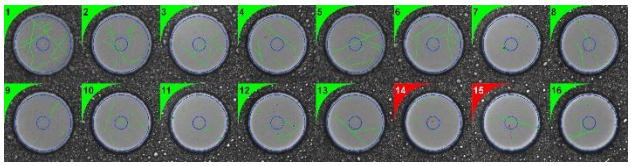

Figure 20. TMT ferrule #12 end face.

In Section 2 it is explained that the MMC connector latching mechanism was designed such that is located far from the ferrule end face so that any debris caused by latching should not be near the fiber faces. In order to investigate the impact of the latch change, six 2x12 MMC and MPO connector mated pairs were terminated and the end faces photographed. Each connector was then mated to a matching like connector 100 times by hand, followed by 4,900 more mates in an automated manner. The automated system was used for efficiency, preceded by 100 hand mates to simulate worst-case mating conditions. No cleaning was performed between any of the mates. After 5,000 total mates, the connectors were all photographed again, cleaned, and photographed one more time to inspect for debris or lasting damage. All of the 12 MMC connectors passed visual inspection outlined in IEC 61300-3-35 [11], while 9 of the 12 MPO connectors failed due to permanent damage after the 5,000 mates. Figure 21 shows a typical MMC connector from the testing in both the initial state, immediately after 5,000 mates with no cleaning, and after cleaning with a standard fiber optic cassette cleaner and compressed air. Figure 22 shows a typical MPO connector under similar conditions, where both more debris is present after the mating test and more permanent damage is visible after cleaning.

The new connector design and latch location of the MMC connector generates less debris than traditional multi-fiber connectors under high-mate conditions.

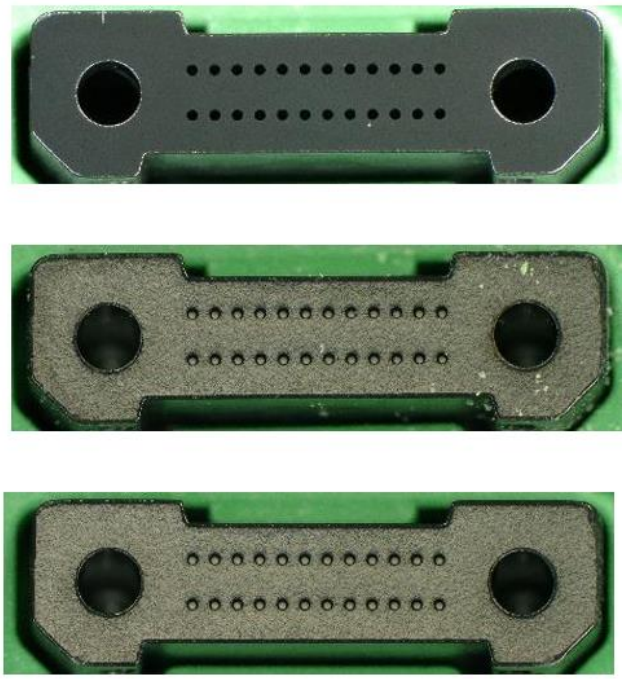

Figure 21. Debris on the end face of an MMC connector: a) initially, b) after 5,000 mates without cleaning, and c) after a final standard clean

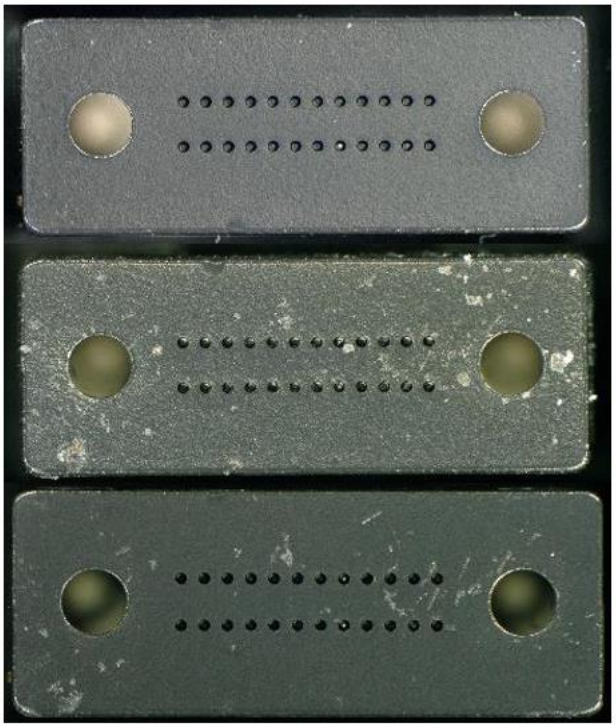

Figure 22. Debris on the end face of an MPO connector: a) initially, b) after 5,000 mates without cleaning, and c) after a final standard clean

7. Conclusions

This paper presents a large dataset of end face geometry and insertion loss testing for the new VSFF MMC connector with TMT ferrule. End face geometry results graded to industry standard MPO 12 fiber connector criteria demonstrate that the new ferrule is capable of achieving the excellent end face geometry and corresponding insertion loss and return loss performance needed for singlemode performance for demanding data center applications. It has been demonstrated that the new connector generates less debris, while the new ferrule is insensitive to ferrule Y-angle deviations beyond IEC EFG specifications.

8. References

[1] D. Childers, J. Hendrick, J. Higley, M. Hughes, D. Kurtz, S. Lutz, D. Schoellner. "A Novel, Low-loss, Multi-Fiber Connector with Increased Usable Fiber Density," International Wire and Cable Connectivity Symposium, (2021).

[2] "Fibre optic interconnecting devices and passive components – Connector optical interfaces, Part 3-31: Connector parameters of non-dispersion shifted single-mode physically contacting fibres – Angled polyphenylene sulphide rectangular ferrules", IEC 61755-3-31, Edition 1.0, June 2015.

[3] "Fibre optic interconnecting devices and passive components – Connector optical interfaces – Part 2-5: Connection parameters of non-dispersion shifted single-mode physically contacting fibres – Angled for reference connection applications", IEC-61754-7-4, Edition 1.0, October 2014.

[4] US Conec Ltd., "MMC Connector Fiber Preparation," PI-1140_MMC-FP, Rev. 1.0, September 2024.

[5] US Conec Ltd., "TMT Ferrule Epoxy Management," PI-1150_MMC-EM, Rev. 1.0, September 2024.

[6] US Conec Ltd., "TMT Ferrule Fiber Installation," PI-1160_MMC-FI, Rev. 1.0, September 2024.

[7] US Conec Ltd., "TMT Ferrule Epoxy Curing," PI-1170_MMC-EC, Rev. 1.0, September 2024.

[8] US Conec Ltd., "TMT Ferrule Polishing Preparation," PI-1180_MMC-EC, Rev. 1.0, September 2024.

[9] US Conec Ltd., "TMT Ferrule Polishing – Domaille Polishing Machine," PI-1190_MMC-POL, Rev. 1.0, September 2024.

[10] H. Asadaa, D. Childers, M. Hughes, T. Ishikawaa, S. Lutz, D. Schoellner, K. Shindoa, Y. Wada. "Next Generation Multi-Fiber Ferrule Using 165 Micron Pitch Optical Fiber," Photonics West Optical Interconnects XXI, SPIE, (2021).

[11] "Fibre optic interconnecting devices and passive components - Basic test and measurement procedures - Part 3-35: Examinations and measurements - Visual inspection of fibre optic connectors and fibre-stub transceivers", IEC 61300-3-35, Edition 3.0, June 2022.

9. Pictures of Authors

Ian Dancel received a Bachelor of Science degree in computer engineering from the United States Military Academy at West Point in 1997. He was involved in telecommunications and network engineering in field and laboratory environments for 19 years prior to joining US Conec in 2016. He is currently focused on fiber optic components as the Process Development Engineering Supervisor at US Conec.

Samuel Field received a Bachelor of Science degree in aerospace engineering from North Carolina State University in 2022. He joined US Conec in 2023 as a Process Development Engineer in the Research and Development Department. He is currently focused on fiber optic components and polishing.

Madison Good received her B.S. in Mechanical Engineering from the University of North Carolina at Charlotte in 2020. Madison joined US Conec in 2021 and is currently focused on process industrialization and customer support as an Applications Engineer.

Michael Kadar-Kallen received a B.S. in Physics and B.A. in Mathematics from the University of Rochester in 1985, and a Ph.D. in Physics from Princeton University in 1992. Michael has been working in the fiber optics industry since 1994, after completing postdoctoral work in atomic physics at Wake Forest University. He is currently a Senior Principal Engineer at US Conec.

Dirk Schoellner received his master's degree in electrical engineering from The Ohio State University. He has been involved in research and development in fiber optics for more than twenty-five years. He joined US Conec, Ltd. in 2007 as a Senior Development Engineer in the Research and Development Department. Currently Dirk is the Manager of Connectivity and Testing at US Conec.

Sharon Lutz has over 22 years of experience in fiber optic interconnects with US Conec and is currently the Product Manager with responsibility over precision optical components. Sharon received her Bachelor of Science degree in Mechanical Engineering from the University of North Carolina at Charlotte in 2004 and her Master of Business Administration from Wake Forest University in 2019. She has been an active member in IEC since 2008 and currently serves as SC86B WG6 convenor.

Charlie Stroup has worked in a variety of engineering roles in the telecommunications industry since 2011. He received a Bachelor of Science in Physics from Guilford College in 2006 and a M.S. in Mechanical Engineering from University of North Carolina at Charlotte in 2008. Charlie has served as a technical expert for WG4 and WG6 of IEC SC86B and is currently the Applications Engineering Manager for US Conec, Ltd.